Geophysical Research Letters

Supporting Information for

Southern Ocean Phytoplankton Blooms Observed by Biogeochemical Floats

T. Uchida[1], D. Balwada[3], R. Abernathey[1,2], C. Prend[4], E. Boss[5] and S. Gille[4]

1: Department of Earth and Environmental Sciences, Columbia University in the City of New York

2: Division of Ocean and Climate Physics, Lamont-Doherty Earth Observatory

3: Center for Atmosphere Ocean Science, Courant Institute of Mathematical Sciences, New York University

4: Scripps Institution of Oceanography, University of California, San Diego

5: School of Marine Sciences, University of Maine

Contents of this file

Introduction

In this document, we provide additional text and time series to supplement the climatologies presented in the main text. Example scripts used for quality control and analyzing the data are given on Github (`doi:10.5281/zenodo.3336575`).

Text S1.

The time series of the one percentile depth of photosynthetically available radiation (PAR) is shown in Fig. S1. Only SOCLIM floats measured PAR and the euphotic-layer depth (h_{Eu}) was defined as the depth above the 0.1 Ein m^{-2} d^{-1} isolume (Mignot et al., 2018).

Text S2.

Figure S2 shows the spread of vertically integrated biomass ($\langle C_p \rangle$) over the whole dataset. The parameters of 200 dbar and 90th percentile were used in our study, but we see that the medians are similar in all cases with lower values than the case with no masking. The last two cases were where we masked out grids that had Chl concentrations lower than 0.01 or 0.02 mg Chl m^{-3}. The values were chosen by inspection from the vertical profiles of Chl.

Text S3.

Figure S3 shows the climatology of absolute dynamical topography (MADT) over the Southern Ocean taken from the AVISO dataset and the magnitude of its horizontal gradient ($|\nabla(\mathbf{MADT})| = [(\partial_x \mathbf{MADT})^2 + (\partial_y \mathbf{MADT})^2]^{1/2}$). The fronts were chosen as isolines of MADT that align with its gradient maxima, similar to Swart et al. (2010). The isoline values were $0, -0.6, -1.03, -1.2, -1.4$ [**m**] respectively. In Fig. S3**a**, we also show the trajectory of the example floats (5904184, 5904683, 5904395). Float 5904184 is south of SBdy, 5904683 drifts eastward along SAF downstream of the Kerguelen Plateau region, and 5904395 is north of the SAF in the Pacific gyre.

Text S4.

Figures S4-S6 show the full time series of the buoyancy frequency (N^2), conservative temperature, absolute salinity, Chl and C_p throughout the entire life cycle of the three example floats (5904184, 5904683, 5904395). Float 5904683 experiences a change in water mass properties indicated by the difference in temperature and salinity between the years 2017 and 2018. Data from 2014-2015 is used in the main text for 5904184, 2016-2017 for 5904683 and 5904395. Figures S7-S9 show the time series of bulk and proxy phytoplankton biomass and accumulation rates from the same three floats.

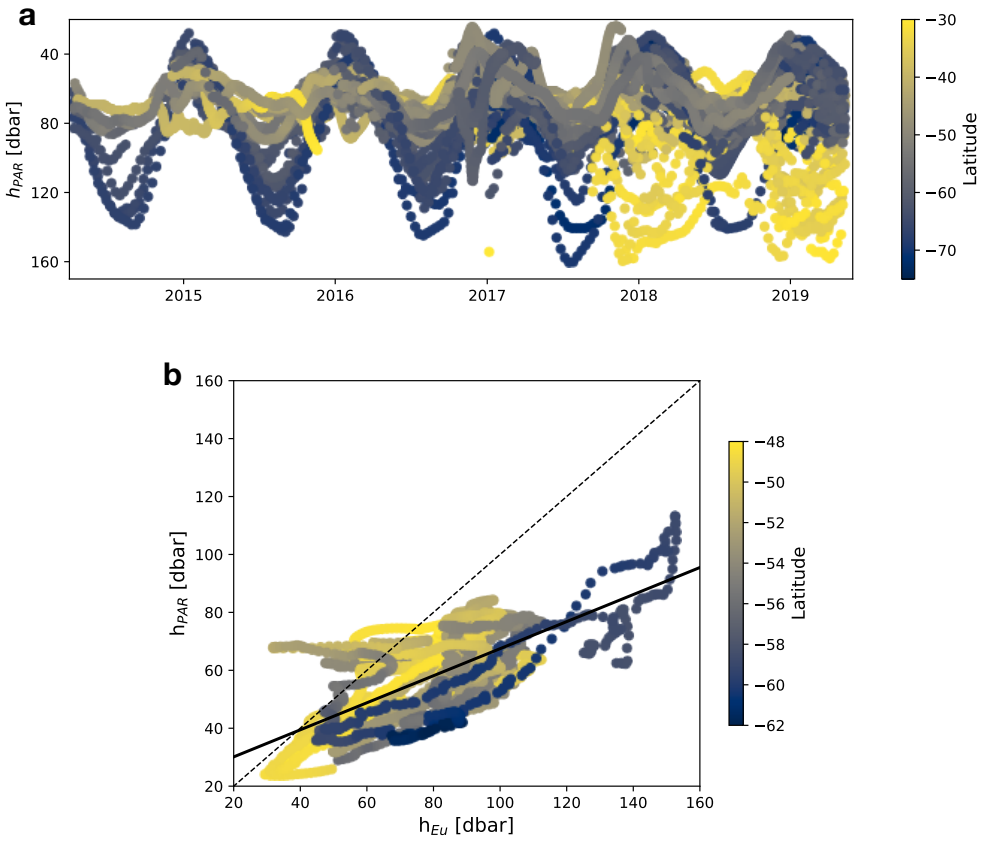

Figure S1. Scatter plot of h_{PAR} from SOCCOM/LIM floats plotted against time **a**. The colors show the corresponding latitude. **b** h_{PAR} plotted against h_{Eu} from the SOCLIM floats. The black dashed line shows the 1-to-1 ratio and solid line the linear regression of $h_{\mathrm{PAR}} \approx 0.47 h_{\mathrm{Eu}} + 20.77$.

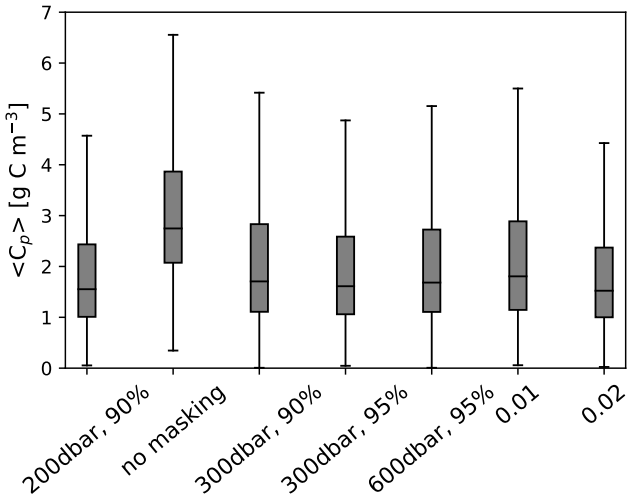

Figure S2. Box plot of $\langle C_p \rangle$ over the whole dataset using different metrics for masking. The median is shown as the black solid line, interquartile ranges as boxes, and the 95 percentile in whiskers.

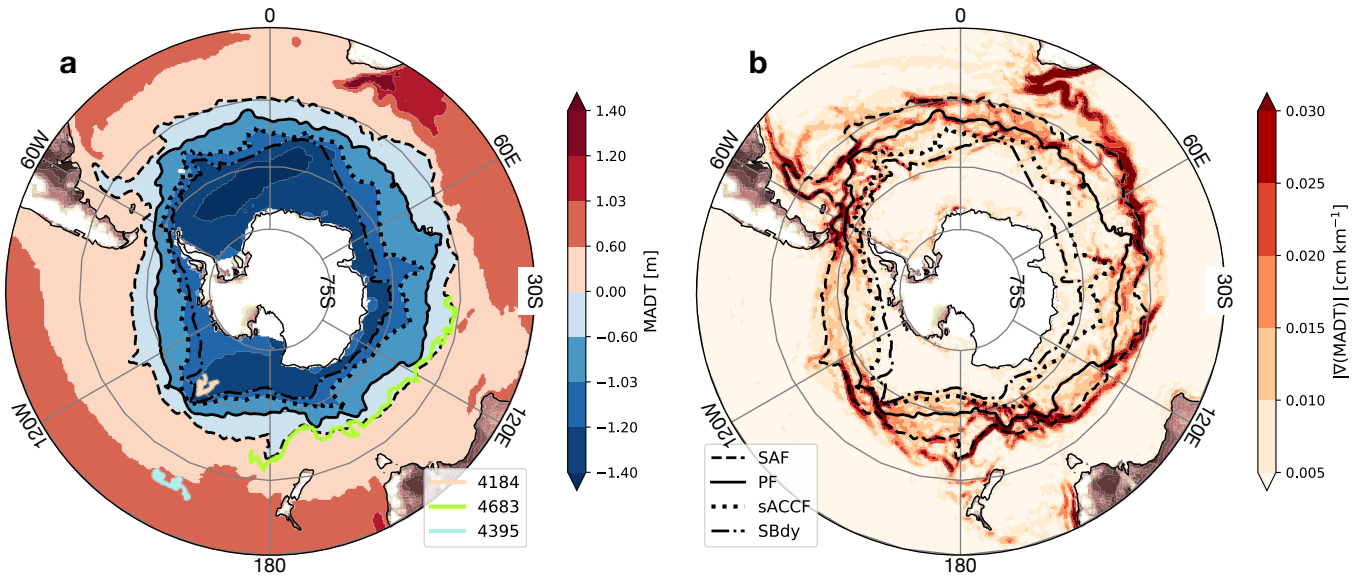

Figure S3. Contour plot of MADT **a** and its horizontal gradient magnitude **b**. On top of them, we also show our MADT-based Subantarctic Front, Polar Front, southern ACC Front, southern boundary of the ACC, and the trajectory of the three example floats.

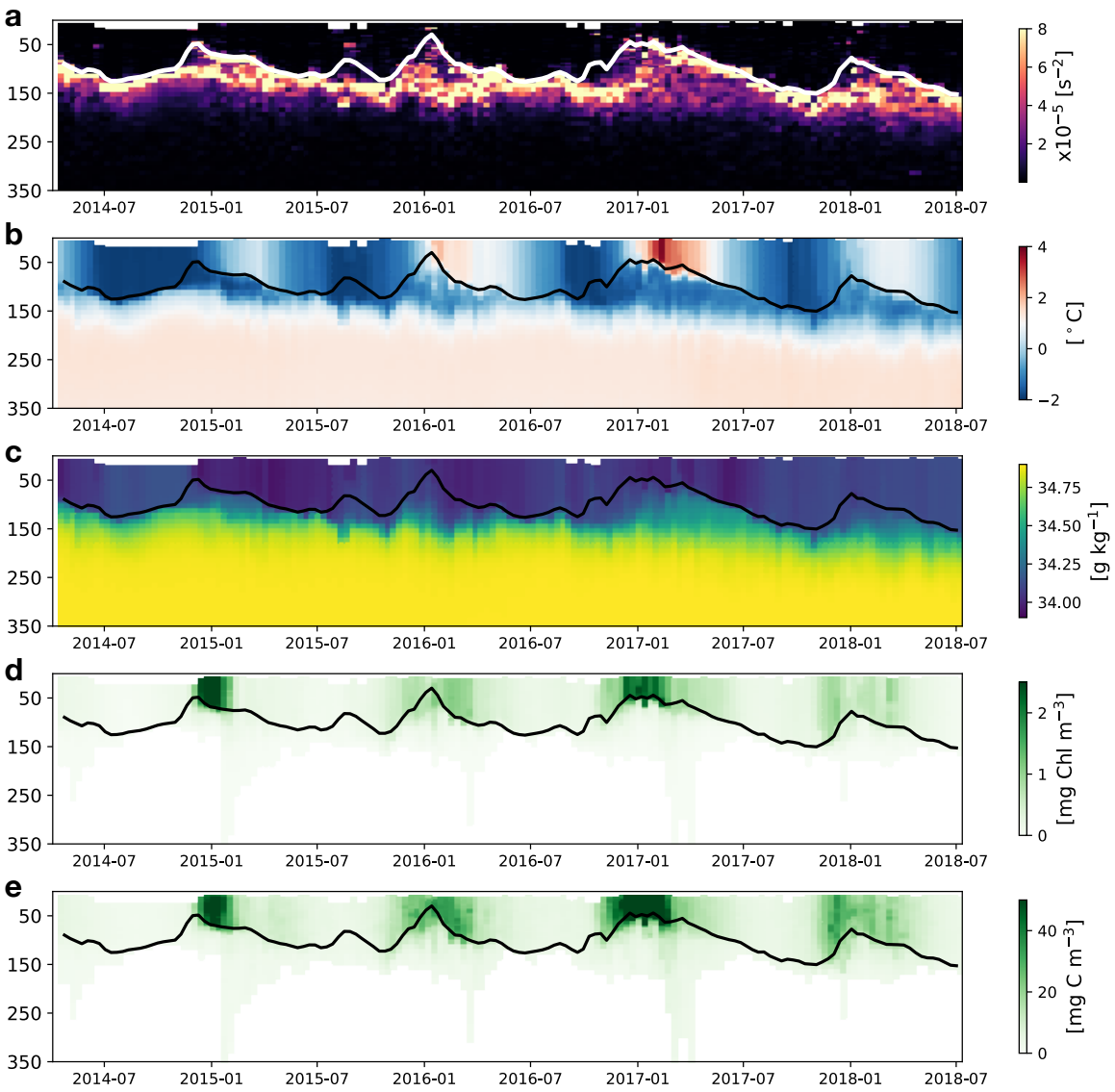

Figure S4. Time series of the stratification (N^2) **a**, conservative temperature **b**, absolute salinity **c**, Chl **d** and C_p **e** from float 5904184. The solid lines show h_{ML}.

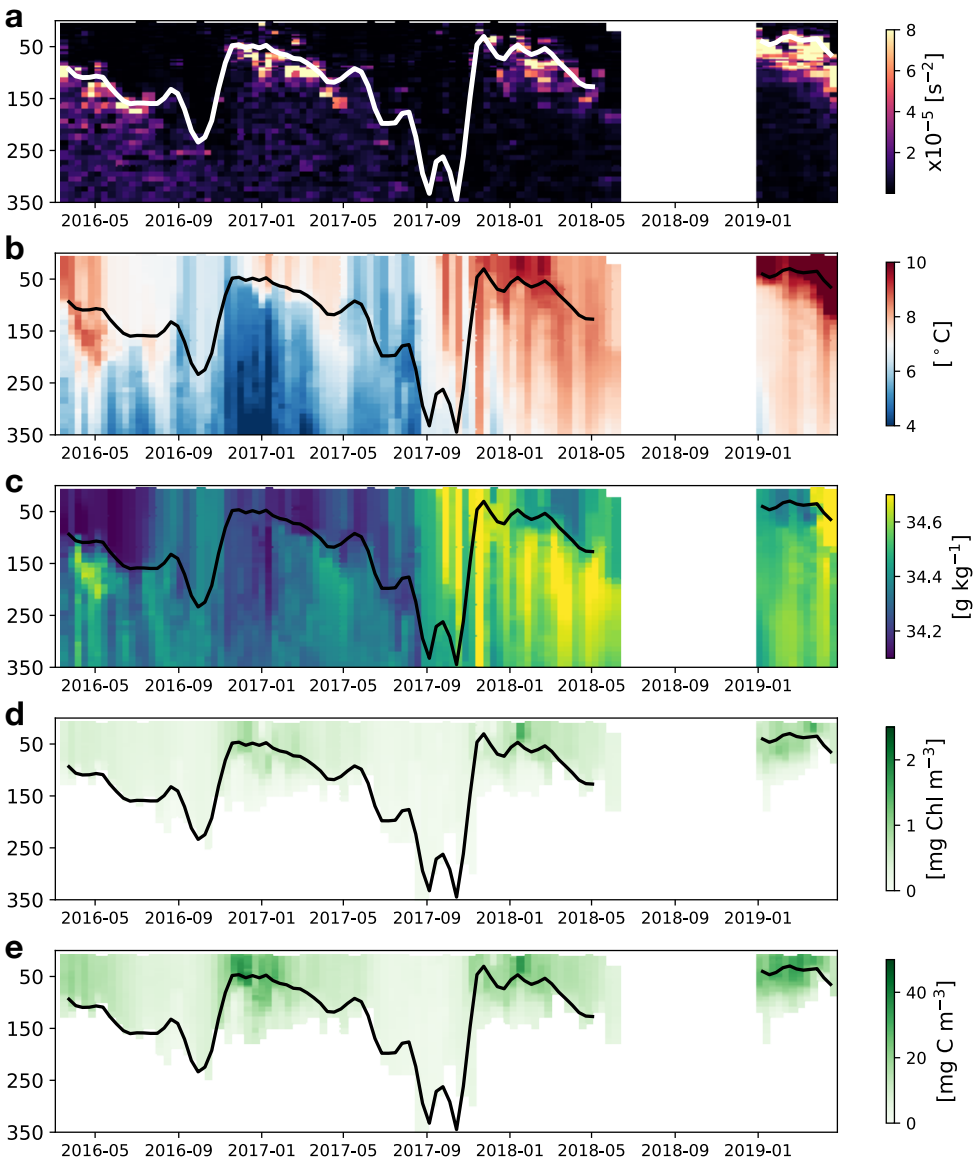

Figure S5. Time series of the stratification (N^2) **a**, conservative temperature **b**, absolute salinity **c**, Chl **d** and C_p **e** from float 5904683. The solid lines show h_{ML}.

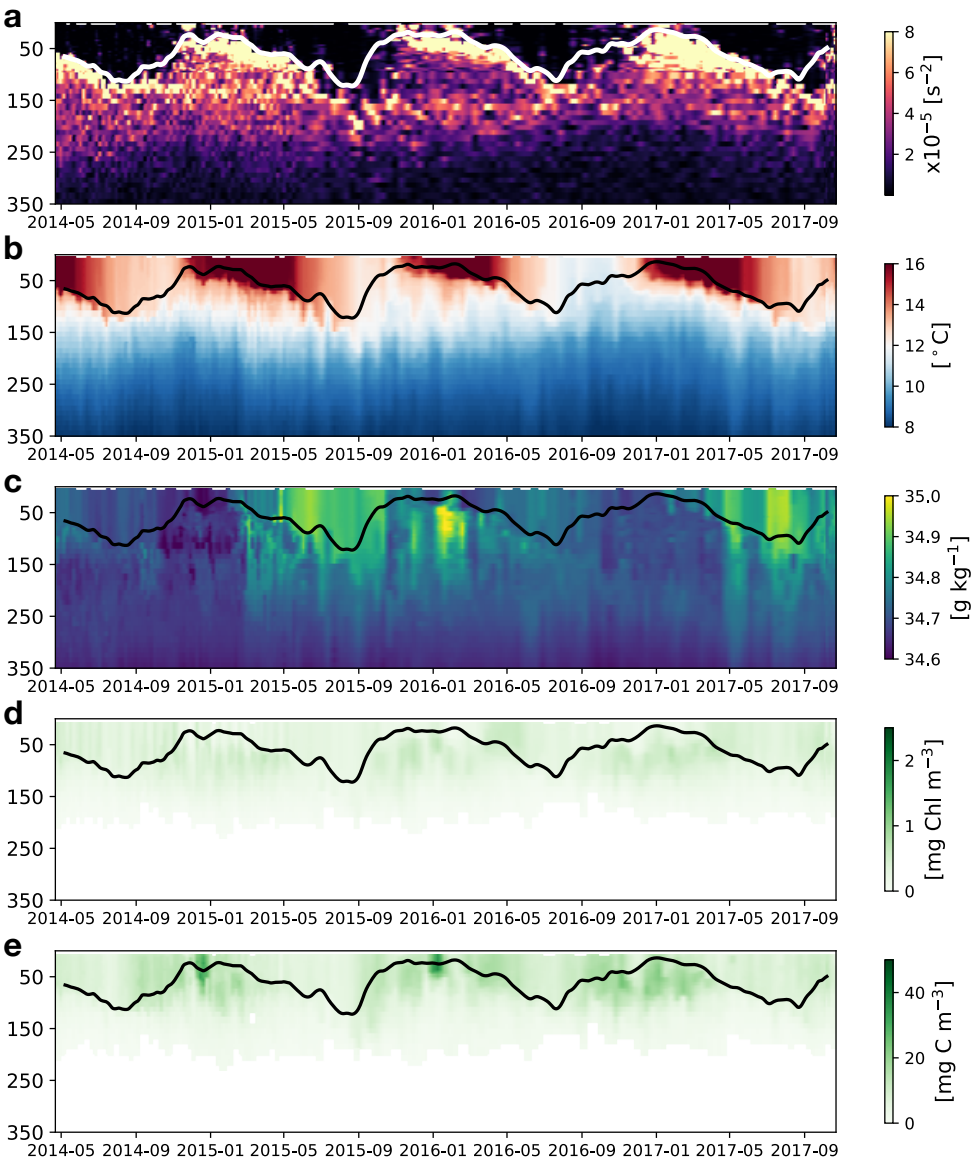

Figure S6. Time series of the stratification (N^2) **a**, conservative temperature **b**, absolute salinity **c**, Chl **d** and C_p **e** from float 5904395. The solid lines show h_{ML}.

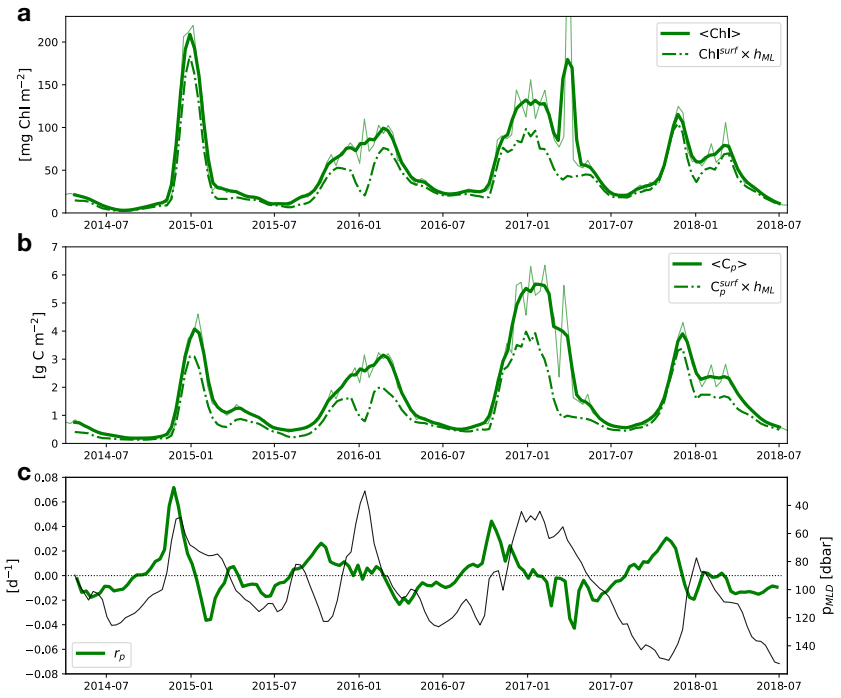

Figure S7. Time series of the vertically integrated Chl ($\langle Chl \rangle$) and surface Chl multiplied by the mixed layer depth **a** and phytoplankton carbon biomass C_p **b** for float 5904184**. c** The accumulation rate (r_p) in green and the mixed-layer depth in black. The thin green lines are before the 30-day running mean is applied.

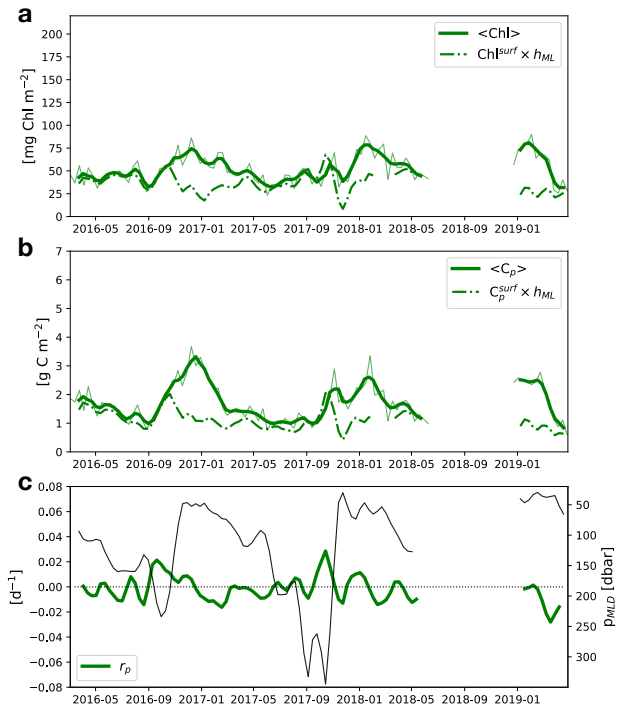

Figure S8. Same as Fig. S7 but for float 5904683.

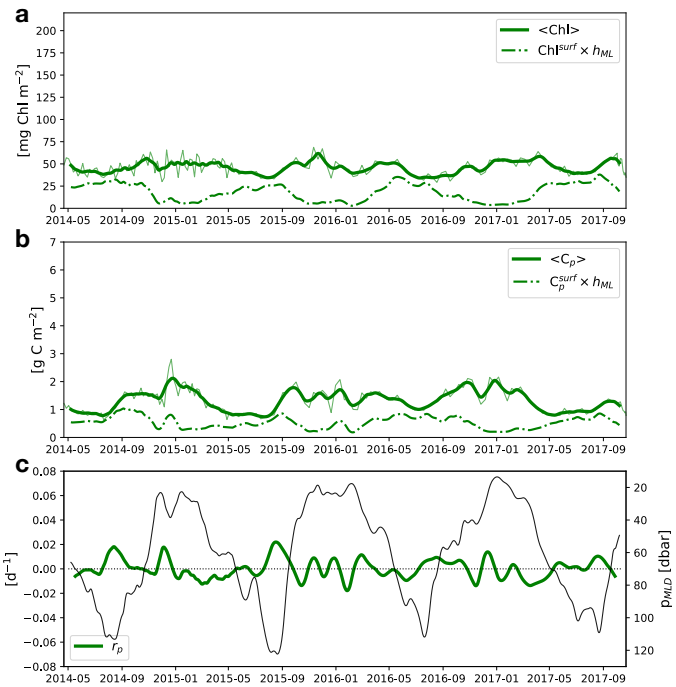

Figure S9. Same as Fig. S7 but for float 5904395.

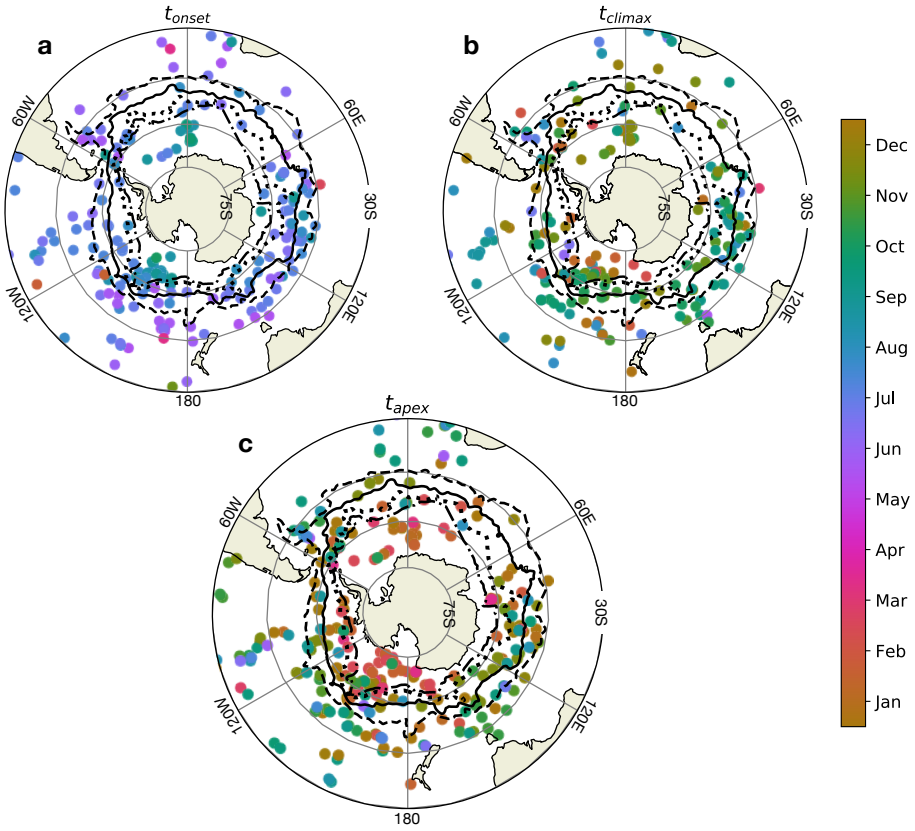

Figure S10. Month in which each spring bloom phase takes place (onset **a**, climax **b**, and apex **c**).

References

Swart, S., Speich, S., Ansorge, I. J., & Lutjeharms, J. R. (2010). An altimetry-based graves empirical mode south of Africa: 1. development and validation. *Journal of Geophysical Research: Oceans*, *115*(C3).

Ardyna, M., Claustre, H., Sallée, J. B., D'Ovidio, F., Gentili, B., Van Dijken, G., Arrigo, K. R. (2017). Delineating environmental control of phytoplankton biomass and phenology in the southern ocean. *Geophysical Research Letters*, *44*(10), 5016–5024.

Mignot, A., Ferrari, R., & Claustre, H. (2018). Floats with bio-optical sensors reveal what processes trigger the north atlantic bloom. *Nature Communications*, *9*(1), 190.